



Published in final edited form as:

*Photochem Photobiol.* 2020 May ; 96(3): 625–635. doi:10.1111/php.13183.

## Pluronic F-127: An Efficient Delivery Vehicle for 3-(1'-hexyloxy)ethyl-3-devinylpyropheophorbide-a (HPPH or Photochlor) †

Joseph Cacaccio<sup>1</sup>, Farukh Durrani<sup>1</sup>, Ravindra R. Cheruku<sup>1</sup>, Ballav Borah<sup>2</sup>, Manivannan Ethirajan<sup>1</sup>, Walter Tabaczynski<sup>2</sup>, Paula Pera<sup>1</sup>, Joseph R. Missert<sup>1</sup>, DR. Ravindra K Pandey<sup>1,\*</sup>

<sup>1</sup>PDT Center, Cell Stress Biology, Roswell Park Cancer Institute, Buffalo, NY 14263

<sup>2</sup>Photolitec, LLC, 73 High Street, Buffalo, NY 14224

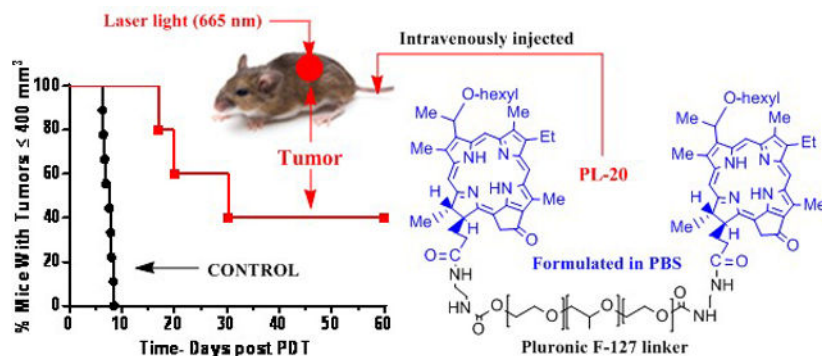
### Abstract

To determine the impact of delivery vehicles in photosensitizing efficacy of HPPH, a hydrophobic photosensitizer was dissolved in various formulations: 1% Tween 80/5% dextrose, Pluronic P-123 and Pluronic F-127 in 0.5, 1 and 2% phosphate buffer solutions (PBS). HPPH was also conjugated to Pluronic F-127 and the resulting conjugate (PL-20) was formulated in PBS. Among the different delivery vehicles, only Pluronic P-123 displayed significant vehicle cytotoxicity whereas Pluronic F127 was non-toxic. Compared to PL-20, HPPH formulated in Tween80 and Pluronic F-127 showed higher cell-uptake, but lower long term retention in Colon26 cell compared to PL-20. The higher retention of PL-20 was similarly observed during *in vivo* uptake with BALB/c mice bearing Ct26 tumors. In contrast to the *in vitro* uptake experiments, PL-20 showed slightly higher uptake compared to HPPH formulated in Tween or Pluronic-F127. A significant difference in pharmacokinetic profile was also observed between the HPPHPluronic formulation and PL-20. Under similar *in vivo* treatment parameters (drug dose 0.47  $\mu\text{mol/kg}$ , light dose: 135  $\text{J/cm}^2$  at 24 h post-injection of PS), HPPH formulated either in Tween or Pluronic F-127 formulation showed similar *in vivo* PDT efficacy (20–30% tumor cure on day 60), whereas PL-20 showed 40% tumor cure (day 60).

### Graphical Abstract

†This article is part of a Special Issue dedicated to Dr. Thomas Dougherty, who devoted nearly five decades of his life to show the use of photodynamic therapy in treating a variety of cancers. His research was truly translational and he played a significant role in the development and approval of Photofrin by several health organizations. Photofrin-PDT is currently being used to treat a variety of cancer patients all over the world. We are grateful to Dr. Dougherty for so many reasons, but perhaps most of all is for the lesson that it is possible to accomplish much when you have the willingness and commitment to work with others, foster relationships near and far, and to persist in the face of obstacles. Above all, he was a great human being. He will be missed by so many, including the PDT community.

\*Corresponding author's ravindra.pandey@roswellpark.org (Ravindra Pandey).



To investigate the impact of delivery vehicles in HPPH-PDT, HPPH was formulated in Tween80, Pluronic F-123, Pluronic F-127 and also conjugated with amino-Pluronic F-127 (PL-20). Among all the formulations, PL-20 in which two molecules of HPPH were conjugated with amino-Pluronic F-127 formulated in PBS showed higher tumor-specificity at long-term tumor cure in BALB/c mice bearing Ct26 tumors.

## INTRODUCTION

Photodynamic Therapy (PDT) is a tri-component process which combines a photosensitizer, light, and oxygen that produces reactive oxygen species, mainly singlet oxygen which causes oxidative stress and the destruction of tumor (1, 2). It is now a well-recognized treatment strategy which is non-invasive and minimally toxic. PDT is also being used to kill viruses (3), microbial cells (4) and bacteria (5). It is also clinically used to treat a wide range of non-oncological medical conditions (6), including treatment of acne (7) and wet, age-related macular degeneration (8).

There are numerous FDA approved photosensitizers (PS) being used in the clinic or are under various stages of preclinical development all over the world (9). A variety of medicinal approaches have been used to develop these PSs, and as a result there are marked differences in their photophysical properties and tumor specificity (10). However, one common characteristic of most porphyrin-based compounds is their high degree of hydrophobicity. The conjugated *pi*-system in tetrapyrrolic systems enables hydrophobic photosensitizers to aggregate, which results in reduced singlet oxygen production (11). However, there are synthetic methods available which could decrease the hydrophobicity while maintaining the PS photophysical properties (10). Ježek et al. (12) investigated the influence of hydrophobicity on the efficacy of a PS (*meso*-tetrakis-phenylporphyrin [TPP]) *in vivo* and have shown that among the compounds investigated, the PS with higher hydrophobicity had a significantly improved cure rate in nude mice with amelanotic melanoma (13). Therefore, while the hydrophobic nature of these compounds makes formulations and delivery a challenge, the biological efficacy increases greatly due to a wide variety of factors such as tumor penetration and decreased clearance from the reticuloendothelial system (14).

For the development of agent(s) with improved tumor-specificity and long-term PDT efficacy, a similar approach has previously been used by us and others to understand the

structure-activity relationship in porphyrins, chlorins, bacteriochlorins and phthalocyanine systems (15–19). Such a study certainly helped in establishing the correlation between overall lipophilicity and PDT efficacy, and identifying the best candidate from each series. Some of the candidates are currently at various stages of clinical and pre-clinical trials (2). The poor water solubility of most of the porphyrin-based PS causes significant problems in clinical development, and the choice of a suitable formulation with limited toxicity is an important step in drug development. A wide variety of formulating agents such as Tween 80, Cremophor, liposomes, microcapsules, microspheres, nanoparticles, nanocrystals and polymers have been explored (20). However, reproducibility, biocompatibility, premature degradation or inactivation within the systemic circulation and toxicity at higher doses are the problems associated with some of these formulations. Therefore, it becomes necessary to investigate the toxicity (including organ toxicity) of these formulating agent(s) before their use in drug formulation.

Current formulations of hydrophobic PS rely on surfactants to stabilize the PS in solution (21). The hydrophobic compounds administered in the clinic are formulated in Cremophor EL or, more recently, Tween 80; both of which can have major adverse effects to the patient. Patients who receive formulations utilizing Cremophor or Tween 80 have had reactions such as hypersensitivity, nephrotoxicity, and neurotoxicity (22). Additionally, Tween 80 has been known to cause anaphylactoid reactions at inject sites in various patients. Therefore, there has been a push to formulate hydrophobic compounds in more biocompatible systems. An attractive alternative for formulating hydrophobic agents has been the use of biodegradable amphiphilic polymers like Pluronic<sup>®</sup> (23). These polymers are comprised of varying amount of ethylene oxide (PEO) and propylene oxide (PPO) moieties arranged in an A-B-A pattern (24). These polymers have the ability to self-assemble into a nanoparticle corona with a hydrophilic PEO forming the shell and the hydrophobic PPO solubilizing the drugs through Van der Waals interactions (25). These nanoparticles can be tuned to optimize size and solubility by changing the nature of Pluronic polymer by varying the number of PEO or PPO moieties.

Drugs formulated in Pluronic have some obvious benefits over Cremophor or Tween 80 which makes it an attractive solubilizing agent (26). For example, (i) the FDA has classified many Pluronic polymers as “Generally Recognized as Safe” (GRAS) which means that developing new formulations utilizing Pluronic will move more quickly through FDA approval, (ii) these polymers do not have the same immunological affects in patients that are seen when using Cremophor or Tween 80, (iii) due to the amphiphilic nature of these polymers, other solubilizing agents (e.g. polyethylene glycols) can be mixed to create sophisticated or highly customizable nanoparticles and finally (iv) these polymers can easily modified making it possible to functionalize or target a nanoparticle to a particular receptor.

Due to these favorable properties, Pluronic formulations are under investigation in clinical trials and increased use in research. Currently, a doxorubicin formulation is under Phase III clinical trial that utilizes a L61/F127 Pluronic mixture to replace the Tween 80 formulation (27). The results from the Phase II trial in patients with advanced adenocarcinoma of the esophagus and gastroesophageal junction demonstrated that the formulation did not display any additional side effects, even possibly reducing the toxic profile of Doxorubicin

(23). Additionally, recent reports showed the benefit of utilizing Pluronic nanoparticles in the administration of Docetaxel (DTX) (28). The current clinical standard for DTX is Taxotere<sup>®</sup>, which utilizes Tween 80 to solubilize the drug. As stated above, Tween 80 has been linked to serious side effects including nephrotoxicity and neurotoxicity. In mice, Fang et al. demonstrated that Docetaxelin Pluronic formulation retained 1.85 times longer than the Tween 80 formulation and had improved *in vivo* efficacy (29). Finally, mixed Pluronic micelle formulations have been investigated in combination with Photofrin (a clinically approved PDT agent) to increase efficacy while decreasing adverse effects like skin sensitivity (30). Among the Pluronic polymers approved by FDA, Pluronic P-123 and Pluronic F-127 have been widely used for formulating a variety of therapeutic agents. Therefore, the objective of this study was to investigate the HPPH delivery ability in both the Pluronic polymers, and compare these results with a Tween 80/5% dextrose formulation.

## MATERIALS AND METHODS

For our study, HPPH was used as a photosensitizer and synthesized by following our own methodology (31).

### Formulation of HPPH.

To investigate the impact of delivery vehicles on biological efficacy of HPPH, it was formulated with Tween 80 or with Pluronic block copolymer surfactants: Pluronic F-127 (avg. mol. wt. 12,600 and Pluronic P-123 (avg. mol. Wt. 5,800) using the following procedures:

(i) HPPH-Tween 80 Formulation: HPPH was formulated in 1% (v/v) and 0.5% (v/v) Tween 80/5% aqueous Dextrose solutions. Approximately 3.8 mg of HPPH was added to a agate mortar. The Tween 80 was added to the HPPH using Wiretrol I micropipettes as follows: for 1% (v/v), 100  $\mu$ L was added, for 0.5%, 50  $\mu$ L was added. Using the agate pestle for 2 to 3 minutes, the mortar contents were mulled to a uniform paste. The pestle was left in the mortar. The mortar and pestle were carefully covered, avoiding contact with the paste with aluminum foil and left overnight.

The next morning, a 0.20 micron syringe filter was attached to the barrel of a 10 mL syringe which was then clamped in a stand with a collection tube under it. For each of the two Tween 80 formulations, a total of 10 mL of 5% Dextrose for injection was added in 3 portions to the mortar; each portion of D5W is mulled in the mortar individually to form a uniform solution which was transferred to the barrel of the syringe filter assembly and filtered. The last portion of the D5W in the mortar was colorless. The filtered solution was mixed well using a vortex mixer. The concentrations of the two Tween 80 solutions were determined spectrophotometrically using the Beer-Lambert equation (extinction coefficient at 660 nm peak in methanol = 47,500 L mol<sup>-1</sup> cm<sup>-1</sup>).

(ii) HPPH in 2%, 1% or 0.5% (w/v), Pluronic F127/DPBS and Pluronic P123/DPBS solutions: In a 100 mL round bottom flask with an egg-shaped magnetic stir bar, approximately 3.5 mg of HPPH was added to 34 mL of 200 proof ethyl alcohol (ACS/USP grade). The flask was capped tightly with foil wrapped by parafilm. The mixture was stirred

for 3 minutes and then sonicated for 5 minutes in a sonicator water bath; temperature of water bath was between 23–27°C. All HPPH was dissolved. The foil cap was removed. Next, Pluronic F-127 or Pluronic P-123 were added as follows: for 2% (w/v), 200 mg of the Pluronic was added to the flask; for 1% (w/v), 100 mg was added; and for 0.5% (w/v), 50 mg was added. Ethyl alcohol (0.2 mL of 200 proof) was used to rinse the test tube used for weighing the Pluronic solid and this was added to the flask. The flask opening was covered tightly with foil wrapped with parafilm. Three cycles of stirring for 5 minutes each and then sonicating for 10 minutes were used to dissolve the Pluronic solid. All solid appeared dissolved as a clear solution.

Next, the ethyl alcohol was removed using a rotary evaporator and high vacuum. To avoid foaming and bumping during this procedure, about 2/3 of the volume of the solution was transferred to another container and the removal of ethyl alcohol was done from the same flask in portions. The temperature of the water bath was kept at <30°C. After all the ethyl alcohol was removed the HPPH/Pluronic mixture appeared as a greyish-white film. The flask and contents were kept under high vacuum connecting the flask to the vacuum pump using a take-off adapter. The next day, while still under vacuum, the flask was placed in a water bath at 30°C for 30 minutes and 8 mL of DPBS (of the total of 10 mL to use) was added to the flask. Using a spatula, the paste was worked into solution with DPBS. The remaining 2 mL of DPBS was used to get any paste off the spatula and was added to the flask solution. The solution in the flask was then alternately stirred and sonicated (3 sets of 3 minutes stirring, followed by 10 minutes of sonication (sonicator bath temperature kept between 22°C – 30°C). The solutions were then filtered – first through a 0.45 micron syringe filter, then through a 0.20 micron syringe filter. The concentration of the solutions were determined spectrophotometrically using the Beer-Lambert equation (extinction coefficient of the 661 nm peak in methanol = 47,500 L mol<sup>-1</sup> cm<sup>-1</sup>), see Scheme 1.

### Synthesis of HPPH-Pluronic F-127 conjugate.

To determine the advantages and limitations of HPPH Pluronic F-127 formulation over HPPH-Pluronic conjugate, HPPH was reacted with amino functionalized Pluronic F-127, which was obtained by following the reported method (32, 33). Amino-Pluronic F-127 powder (0.33 eq, 0.0238 mmol) and HPPH (1 eq, 0.0712 mmol) were dissolved in anhydrous DCM (8 mL), followed by the addition of EDC (2 eq, 0.157 mmol) and DMAP (catalytic amount, 20 mg) while the PF-127 was dissolved in DCM via vigorous stirring. After allowing the PF-127 and HPPH solutions to completely dissolve, they were mixed slowly, and the reaction mixture was gently stirred for 48 h at room temperature. The reaction mixture was evaporated and residue is dried well (Scheme 2). This crude material/water dissolved in water (8 mL) and was dialyzed (*Slide-A-Lyzer* MW cut-off: 10000 Da) for 2 days against distilled water to remove unconjugated HPPH and DCM. The final solution was lyophilized. The powder was dissolved in minimum amount of methanol and purified by chromatography using a gravity column filled with Sephadex LH-20 (Sigma-Aldrich, Co.) as stationary phase, and methanol/water served as the mobile phase. A 4.0 g portion of the Sephadex LH-20 was dissolved in 10 mL of methanol for activation, applied to a chromatographic column (2 × 60 cm) packed with LH-20. After loading the crude product, the column was run at a flow rate of 0.5 mL/min, with the mobile phase starting

from 50% methanol / 50 % water (0–60 min), and proceeding to 80% methanol / 20 % water (61–110 min). The major fraction was collected, the solvent was evaporated and the structure was confirmed by NMR and mass spectrometry analyses.

### **Size of HPPH formulations by dynamic light scattering (DLS).**

DLS measures the hydrodynamic diameter, which takes into account the surface modification when calculating mean diameter; the mean diameter from DLS compared to electron microscopy should be higher. The increase in mean diameter is also dependent on the bulkiness of the post-loading. Measurement of hydrodynamic size provides information about the solvent layer that assembles around the nanoparticles; a larger apparent diameter indicates a greater ability to arrange a corona of solvent molecules around the nanoparticle, and such nanoparticles are likely to have a higher Zeta potential and are more likely to remain dispersed over time. The DLS measurements were performed on a Nicomp 370 Submicron Particle Sizer (Nicomp, Santa Barbara, California). The NP solution was placed in a borosilicate glass capillary tube, and diluted with water to an intensity reading of 300 kHz. The readings were performed in triplicate with each run set for 5 minutes. DLS was performed on loaded and unloaded nanoparticles dispersed in 1% Tween 80 water to determine their hydrodynamic diameter. NICOMP proprietary software was used to measure the sizes of different populations in the polydispersed samples. Samples were syringe filtered through a 0.2 micron filter and immediately analyzed. Two runs of 5 minutes each were collected. The volume-weighted analysis was chosen as the most representative measurement of hydrodynamic size.

### **Cell line.**

The *in vitro* studies (cell uptake, PDT efficacy by MTT assay, intracellular localization and comparative cell specificity at various time points) were performed in Ct26 cells. This cell line has been extensively studied in our lab so the *in vitro* and *in vivo* effects of HPPH formulated in Tween 80 solution are well known. Ct26 cells were purchased from American Type Culture Collection (ATCC, Manassas, VA). The cells were maintained in DMEM supplemented with 10% FBS, 100 i.u. penicillin and 100 mg/mL streptomycin in 5% CO<sub>2</sub> at 37°C.

### **Intrinsic cytotoxic effect of Pluronic vehicle solutions.**

In order to investigate the influence of the vehicle on the intrinsic toxicity of the formulating solution, a MTT cytotoxicity assay with no light exposure was performed on solutions of Pluronic P-123 in DPBS (at 0.5 %, 1.0% and 2.0% ( w/v) and Pluronic F-127 at 0.5 %, 1.0% and 2.0% (w/v) with no light exposure.

### **In vitro PDT efficacy of HPPH formulations.**

The *in vitro* PDT efficacy of HPPH formulated either in 1%, 2%, or 0.5% Pluronic F-127 and the HPPH-Pluronic conjugate (PL-20) dissolved in PBS was determined by incubating in Ct26 cells at variable concentrations of PS for 24 hours. The cells were then washed, exposed to light at 665 nm, 1.0 J/cm<sup>2</sup>. After 48h, a MTT assay was performed and cell viability was determined.



### **Intracellular uptake and retention of HPPH and subcellular localization of HPPH.**

To determine the cell uptake of PL-20 and HPPH-Pluronic F-127 formulations, the Colon26 cells were plated at  $3 \times 10^5$  cells in a 6 well plate and allowed to adhere. After 24h, the PSs were added (conc. 1  $\mu$ M) and incubated for 24 hours. The cells were then washed with PBS, the media was replaced and the cells were visualized with a Zeiss fluorescent microscope. The images were analyzed using ImageJ to calculate the grey value per cell for the field in triplicate. 24 hours after the first image was taken, the cells were washed again with PBS and imaged.

To determine the sub-cellular localization of the formulations, Colon26 cells were plated at  $1 \times 10^6$  cells in a 6 well plate. After 24h, the HPPH formulations (conc. 1  $\mu$ M) were added after 24 hours along with lysosome and mitochondria probes (Fluospheres and Mitotracker red respectively). The cells were harvested and run on an Image Stream to determine the bright detail similarity for the mitochondria and lysosomes.

### **In vivo tumor-uptake and PDT efficacy.**

The tumor-uptake of HPPH formulated in 2 % Pluronic F-127 / DPBS and the HPPH-Pluronic F-127 conjugate were investigated. The *in vivo* PDT efficacy was investigated for: HPPH formulated in Tween 80, HPPH formulated in Pluronic F-127 / DPBS and of the HPPH-Pluronic F-127 conjugate formulated in DPBS. BALB/c mice bearing Ct26 tumors were used following a standard approach. Three sets of BALB/c mice (female), 5 mice/group/set bearing Colon26 tumors, size 65 mm<sup>3</sup>, were injected intravenously with HPPH in 1% Tween 80 / D5W (1<sup>st</sup> set); HPPH in Pluronic F-127 / DPBS (2<sup>nd</sup> set); and HPPH-Pluronic conjugate PL-20 in DPBS (3<sup>rd</sup> set). The tumors were exposed to light (135 J/cm<sup>2</sup>/75 mW/cm<sup>2</sup>) at 24h post-injection (the optimal time of tumor uptake). The tumor volume  $V = (L \times W^2) \times 0.5$  (L = length – longest dimension) and W = width (perpendicular to the long axis) was measured with calipers. The hours-to-end-point (THE) time for tumors to grow 400 mm<sup>3</sup> was calculated by linear interpolation using Microsoft Excel based software. Mice were sacrificed if and when tumor reached the end point (400 mm<sup>3</sup>). For each group a Kaplan-Meier curve was generated (using Prism4, GraphPad Software Inc.) and the medium Kaplan-Meier tumor growth THE time was estimated. To test for significant differences between pairs of the curves, the Cox-Mentel test was used. These studies were performed following the protocol approved by the Institute's IACUC committee.

### **UV-visible and fluorescence measurements.**

The electronic absorption spectra of HPPH and PL-20 were obtained in organic solution (methanol) and aqueous solution (17% fetal bovine serum in DPBS) using a Cary Bio50 Spectrophotometer. Fluorescence emission spectra of these compounds were also obtained in methanol and 17% fetal bovine serum in DPBS using a Cary Eclipse Fluorescence Spectrophotometer.

The UV-visible absorption spectra and fluorescence emission spectra of the formulated solutions of HPPH in 1% Tween 80, 2% Pluronic F-127, 2% Pluronic P-123 and of PL-20 in DPBS which were diluted in methanol and in 17% FBS in DPBS were also obtained.

## RESULTS AND DISCUSSION

### Characterization of HPPH-Pluronic F-127 conjugate

The  $^1\text{H}$  NMR spectrum (Figure 1) of PL-20 is generally consistent with the proposed structure. The presence of two amide NH signals ( $\delta = 5.28$  and  $6.03$  ppm) provides evidence supporting conjugation. Most proton signals of the photosensitizers (PS) were seen at the expected chemical shifts and intensities. Some, however, were not clearly observed due to overlap with large signals, like those of the Pluronic moiety. The broad, intense signals ( $\delta \sim 3.5$  ppm) of the Pluronic methylene and methine groups obscured the PS signals (i.e.  $8\text{-CH}_2\text{CH}_3$ , ring  $\text{CH}_3$  and  $\text{-OCH}_2(\text{CH}_2)_4\text{CH}_3$ ) normally seen in this chemical shift range. Similarly, one of the  $17\text{-CH}_2\text{CH}_2$ -group protons was not observed, likely due to interference from larger peaks in the crowded spectral region at  $\sim 2.0$  ppm. Overlap was less severe in the region containing the Pluronic methyl signals ( $\delta \sim 1.1$  ppm). Although PS signals near this shift were more clearly observed, their integrated intensities were affected. The severity of the peak overlap is illustrated by comparing the proton spectra of the free PS and the conjugate (Figure 1). Most aspects of the proton spectrum showed a general agreement with structure, including the signals generated by the Pluronic moiety. However, proton signals of the Pluronic moiety of PL-20 were somewhat more intense than expected. The methylene and methine signals resonating at  $\sim 3.5$  ppm were expected to exhibit an integrated intensity of 995 protons. After adjusting for additional (PS and linker) signals found at approximately this chemical shift, the sum of the observed integrated intensity for the Pluronic methylene and methine signals was 1,144 protons. A similar surplus of protons was seen for the Pluronic methyl signals. We expected 195 protons, but observed 212 protons. Since Pluronic F-127 is polymeric, we suggest that this  $\sim 10\text{--}15\%$  excess is due to a difference between the actual and nominal average chain lengths. That is, we believe the actual number of repeats of the monomeric units comprising our starting material (Pluronic F-127) was somewhat larger than specified, resulting in the higher than expected integrated intensity.

**$^1\text{H}$  NMR (400 MHz,  $\text{CDCl}_3$ ),  $\delta$  ppm).**— 9.78/9.75 (2H, s, 2 x PS 5-H), 9.50 (2H, s, 2 x PS 10-H), 8.51 (2H, s, 2 x PS 20-H), 6.03 (2H, br s, 2 x amide NH), 5.90/5.88 (2H, q,  $J = 6.7$  Hz, 2 x PS  $3^1\text{-H}$ ), 5.28 (2H, br s, 2 x amide NH), 5.27 (2H, d,  $J = 19.6$  Hz, 2 x PS  $13^2\text{-CHH}$ ), 5.10 (2H, d,  $J = 19.7$  Hz, 2 x PS  $13^2\text{-CHH}$ ), 4.50 (2H, q,  $J = 7.3$  Hz, 2 x PS 18-H), 4.33 (2H, m, 2 x PS 17-H),  $\sim 2.75\text{--}4.26$  (\*1178H, br m, 4H for 2 x PS  $8\text{-CH}_2\text{CH}_3$ , 4H for 2 x PS  $\text{-OCH}_2(\text{CH}_2)_4\text{CH}_3$ , 18H for 6 x PS ring  $\text{CH}_3$ , 8H for 2 x  $\text{-NHCH}_2\text{CH}_2\text{NH-}$ , 1144H for all Pluronic CH &  $\text{CH}_2$  groups), 2.66 (2H, m, 2 x 1H of PS  $17\text{-CH}_2\text{CH}_2\text{-}$ ), 2.39 (2H, m, 2 x 1H of PS  $17\text{-CH}_2\text{CH}_2\text{-}$ ), 2.24 (2H, m, 2 x 1H of PS  $17\text{-CH}_2\text{CH}_2\text{-}$ ), 2.09 (6H, d,  $J = 6.5$  Hz, 2 x PS  $3^1\text{-CH}_3$ ), 1.79 (6H, d,  $J = 7.2$  Hz, 2 x PS 18- $\text{CH}_3$ ),  $\sim 1.72$  (4H, br m, 2 x PS  $\text{-OCH}_2\text{CH}_2(\text{CH}_2)_3\text{CH}_3$ ), 1.70 (6H, t,  $J = 7.5$  Hz, 2 x PS  $8\text{-CH}_2\text{CH}_3$ ), 1.27–1.48 (4H, m, 2 x PS  $\text{-O}(\text{CH}_2)_2\text{CH}_2(\text{CH}_2)_2\text{CH}_3$ ), 1.21 (8H, m, 2 x PS  $\text{-O}(\text{CH}_2)_3(\text{CH}_2)_2\text{CH}_3$ ), 1.13 (212H, m, all Pluronic  $\text{CH}_3$  groups), 0.77 (6H, t,  $J \sim 6.4$  Hz, 2 x PS  $\text{-O}(\text{CH}_2)_5\text{CH}_3$ ), 0.44 (2H, br s, 2 x PS core NH),  $-1.73$  (2H, br s, 2 x PS core NH). Two protons of the (2 x 1H of  $17\text{-CH}_2\text{CH}_2\text{-}$ ) were not observed, presumably because of overlap with larger signals found nearby, in the crowded spectral region at  $\sim 2.0$  ppm. Integrated peak areas observed in these regions ( $\sim 2.75\text{--}4.26$  and  $\sim 1.13$  ppm) were higher than expected. This was presumed to be due to a difference in chain length (actual vs. expected) of the Pluronic moiety. Integrated



intensities were expected to be 995H for the Pluronic CH and CH<sub>2</sub> groups at ~3.6 ppm, and 195H for Pluronic CH<sub>3</sub> groups at ~1.1 ppm.

### Particle size of HPPH formulations and HPPH-Pluronic-127 conjugate by DLS

The hydrodynamic size plays a role in localization within the body after dosing; nanoparticles below ~150 nm have a prolonged half-life in circulation due to slower uptake by macrophages (34), and size-dependent interactions with cell membranes and across physiological drug barriers determine uptake of nanoparticles. The DLS profiles of the HPPH-Pluronic conjugate in DPBS and HPPH in Tween 80/D5W and Pluronic F-127/DPBS formulations are shown in Figure 2.

### Impact of delivery vehicles on Zeta potential

The Zeta potential was determined using a dynamic light scattering instrument and Zeta Potential software (Brookhaven Instruments, Holtsville, New York) and the results are shown in Figure 3. Nanoparticles were dispersed by vortexing and sonication in 1% Tween 80 in water at 0.2 mg/mL, passed through a 0.2 micron filter and measured in ten replicates. The formulations were filtered through a 0.2 microm syringe filter and immediately read on a Zeta Potential instrument using NICOMP proprietary software. The 2% Pluronic F-127 blank solution had a Zeta potential near 0.0 mV, which means it might begin to flocculate in aqueous solutions after a short period of time; the HPPH-Pluronic conjugate and HPPH-Pluronic F-127 formulation had Zeta potentials of +97.57 mV and +100.17 mV respectively, which suggests that these particles may behave more as a colloidal suspension, repelling like-charged particles and staying dispersed for a longer period of time.

### Absorption and fluorescence characteristics of HPPH and PL-20

The absorption and fluorescence spectra of HPPH and PL-20 were measured in methanol at equimolar concentrations (Figure 4). The absorption peaks of PL-20 across the spectrum were approximately 2-fold higher than those for HPPH. Otherwise, the spectral profiles of the two compounds were the same. Excitation of both the compounds exhibited a strong fluorescence emission at 670 nm with a shoulder band with less fluorescence at 720 nm, but the fluorescence intensity of PL-20 was approximately 2-fold higher than HPPH.

### *In vitro* studies

**Selection of delivery vehicle.**—For the selection of best Pluronic polymer to formulate HPPH, the cytotoxicity of P-123 and F-127 Pluronic polymers was investigated at different concentrations (0.5, 1.0 and 2.0% (w/v) Pluronic in PBS). As can be seen in Figure 5, the Pluronic P-123 solution was intrinsically cytotoxic at the 1% and 2 % concentration levels. While reducing the w/v% of P-123 to 0.5% reduced the observed toxicity, there was significant precipitation when left in refrigerator for longer than a week. The Pluronic F-127 solutions were not cytotoxic from 0.5% to 2.0%. Therefore, the FDA approved Pluronic F-127 was selected for further studies. HPPH was formulated in three concentrations of Pluronic F-127: 0.5, 1.0 and 2.0% (w/v). The solubility of HPPH in Pluronic F-127 formulations over the timeframe when stored at -20°C, 4°C and at room temperature was

maintained. Therefore, HPPH was formulated in Pluronic F-127 and its biological efficacy was compared with Tween 80 formulation and PL-20.

**Impact of delivery vehicles in *in vitro* PDT efficacy of HPPH.**—The *in vitro* PDT efficacies of HPPH formulated in Pluronic F-127, Tween 80 and conjugated with Pluronic F-127 (PL-20) were determined by MTT assay (35) in Ct26 tumor cells. The cells were incubated with HPPH formulations (Tween 80 and Pluronic) and PL-20 in PBS at the concentrations ranging from 12.5 to 1600 nM for 24h, and then exposed to a light at 665 nm at a dose of 1 J/cm<sup>2</sup>. Cell survival was determined 48h after light treatment by MTT assay. The experiments were performed in triplicates and the combined results shown in Figure 6 indicate that HPPH formulated in the various Pluronic F-127 formulations (0.5, 1 and 2%) showed similar efficacy, and was more effective than its Tween 80 formulation. Interestingly, under similar treatment parameters the PL-20 in which two molecules of HPPH conjugated with Pluronic F-127 was the least effective (Figure 6). The lower *in vitro* PDT efficacy of PL-20 could be due to its lower uptake in tumor cells or reduced singlet oxygen producing ability under physiological conditions. Therefore, before evaluating these formulations *in vivo*, the following *in vitro* experiments were performed.

**Comparative cell-uptake, intracellular localization, cell-specificity and retention of HPPH formulated in Pluronic F127 and HPPH-Pluronic conjugate (PL-20).**—The hydrophobic photosensitizers tend to aggregate in certain formulations, which causes intramolecular energy and/or electron transfer between the molecules resulting in reduced singlet oxygen yield and photosensitizing efficacy when exposed with an appropriate wavelength of light. The aggregation of a photosensitizer in solution/formulation can be assessed by measuring the fluorescence in PBS with 17% FBS (physiological conditions) and comparing these values to the fluorescence of the PS measured in methanol (dis-aggregated form).

The fluorescence emission scans of the conjugate PL-20 and of HPPH formulated in Tween 80 and Pluronic F-127 solutions diluted in methanol (organic) and 17% FBS/DPBS (aqueous) are shown in Figures 7A and 7B. Reduced fluorescence intensity of a photosensitizer solution diluted with 17 % FBS/DPBS compared to its fluorescence intensity when diluted in methanol indicates a higher degree of aggregation in an aqueous environment. The fluorescence intensities in organic and aqueous dilution of HPPH formulated in Pluronic F-127 are approximately the same. For HPPH formulated in Tween 80 the fluorescence intensity in aqueous dilution is 4-fold less than its intensity in organic dilution. The fluorescence intensity of PL-20 solution diluted in aqueous solution is half the fluorescence compared to its dilution in organic solvent.

Our next step was to investigate a correlation between the cell-uptake of these formulations to their PDT efficacy. To determine the uptake of each formulation, Colon26 cells were incubated in 6-well plates with the photosensitizer for 24 hours. After 24 hours, cells were washed with PBS and the plates were observed under a fluorescence microscope. The grey value of the fluorescence image was calculated using ImageJ and then normalized to the number of cells in the image and the results are shown in Figure 8. Both Tween 80 and F-127 formulations of HPPH had similar uptake per cell but PL-20 gave significantly lower

uptake (Figure 8). Interestingly the images of PL-20 in the cell show a high degree of granulation. This granulation could be due to PL-20 interaction with membranes creating clusters of photosensitizers on different organelles (see Figure S1, Supporting Information). Additionally, 24 hours after the cells were washed with PBS, only PL-20 remained in the cells at level to be detected microscopically, and a direct correlation between the cell-uptake and *in vitro* PDT efficacy of HPPH formulations was observed.

It has been shown that the intracellular localization of a PS to organelles and other cellular structures make a significant difference on the cytotoxicity and the mechanism of PDT (36). The amount of photosensitized damage to cell functions whose localization in the cells is known gives information about the intracellular localization of the PS. Fluorescence microscopy is the most direct method and has been used extensively because most photosensitizers have the inherent ability to fluoresce. Except for a few examples (37), the most of the porphyrin-based PS localize either in mitochondria or lysosomes (38, 39). To investigate the impact of formulations in mitochondrial and lysosomal localization ability, HPPH formulated in Tween 80, Pluronic F-127 and conjugated with Pluronic 127 (PL-20) was investigated by using the site-specific probes. The results shown in Figure 9 suggest that the HPPH formulated in Tween 80 or Pluronic F-127 show a slight preference for mitochondria over lysosomes, whereas PL-20 shows a significant preference to mitochondria than lysosomes.

### ***In vivo* studies**

Photodynamic therapy treatment requires three components: (i) photosensitizer, (ii) oxygen and (iii) light, and for optimizing the treatment parameters it becomes necessary to determine the time for maximal uptake of the PS in tumor after injection, which may vary from tumor to tumor type due to a significant difference in tumor morphology and vascularity (40) and it may also correlate with the normal oxygen content, required for producing sufficient singlet oxygen, a key cytotoxic agent for the destruction of tumor. To compare the *in vivo* efficacy of HPPH either formulated or conjugated in Pluronic F-127, the following studies were performed.

**Tumor uptake of HPPH-Pluronic formulation vs PL-20.**—The *in vivo* uptake/biodistribution of HPPH formulated in Pluronic F-127 was compared with PL-20 (HPPH conjugated with Pluronic F-127) in BALB/c mice bearing Colon26 at various time points (Figure 10). In brief, tumored mice (3 mice/group/PS) were injected with the PS formulations PS dose (0.47  $\mu\text{mol/kg}$ ), and were imaged at 24, 48, 72 and 96h post-injection. The PS uptake in tumor, liver and skin was measured by IVIS Spectrum (excitation: 675 nm, emission: 720 nm). The results presented in Figure 10 show a significant difference in tumor uptake and retention of the PS in two formulations. For example, HPPH formulated in Pluronic F-127 showed high tumor uptake between 4 to 24h post injection, whereas PL-20 (HPPH-Pluronic conjugate) produced optimal uptake at 24–72h post-injection with minimal skin uptake. The ratio of HPPH uptake between the tumor and liver was approximately 5 to 1, whereas HPPH formulated in Pluronic-127 showed less tumor specificity with a ratio of only 1.3 to 1 between the tumor and liver. Interestingly, the HPPH showed much faster clearance from all the organs in Pluronic formulation than the corresponding Pluronic

conjugate, the mice in both formulations did not show any abnormal behavior, distress or toxicity. However, the fluorescence intensity of HPPH in PL-20 is 2-fold higher than Pluronic F-127 formulation. Therefore, the total amount of PS present in tumor in both the formulations is almost same.

**Comparative PDT efficacy of HPPH-Pluronic formulation vs PL-20.**—The *in vivo* PDT efficacies of HPPH formulated in 2% Pluronic-F127 and HPPH-conjugated with Pluronic-F127 (PL-20) were investigated in BALB/c mice bearing Ct26 tumor (5–10 mice/group). The female BALB/c mice 6–8 weeks of age were subcutaneously injected with Ct26 cells ( $1 \times 10^6$ ), implanted on the flank and left to grow to 4–5 mm diameter. Mice were then injected with 0.47  $\mu\text{mol/kg}$  of HPPH formulated either in 2% Pluronic F-127/PBS or conjugated with Pluronic F-127 (PL-20). At 24h post-injection, the time of maximal tumor uptake of the PS, the tumors were irradiated with light (665 nm, 135  $\text{J/cm}^2$  and a fluence rate of 75  $\text{mW/cm}^2$ ), and the tumor regrowth was monitored for 60 days. Tumor volume was calculated as length x width x  $\frac{1}{2}$  width. The HPPH formulated in 2% Pluronic F-127 gave or in Tween 80 gave 20–30% tumor cure, whereas at the same treatment parameters 40% long-term cure was observed with PL-20. The preliminary *in vivo* tumor efficacy results are shown in Figure 11.

## CONCLUSIONS

In summary, the results obtained from the *in vitro* and *in vivo* studies of HPPH formulated in various formulations show a significant difference in cell-uptake and biological efficacy. Interestingly, compared to HPPH formulated in Tween 80 and Pluronic F-127, PL-20 in which two molecules of HPPH are conjugated with Pluronic F-127 showed comparatively lower cell-uptake and cell-kill (Colon26 tumor cells) *in vitro*. However, PL-20 under similar treatment parameters produced higher *in vivo* PDT efficacy than other HPPH formulations in BALB/c mice bearing Colon26 tumors. Such a difference between *in vitro* and *in vivo* results of PL-20 could be due to its less aggregation *in vivo*, resulting in higher singlet oxygen production. Further studies to confirm the utility of this methodology in developing improved PDT agents with desired photophysical properties are currently underway. This approach could be extremely useful in designing water-soluble cancer-imaging and therapy agents with high tumor-specificity.

## Supplementary Material

Refer to Web version on PubMed Central for supplementary material.

## Acknowledgements

The financial support received from the NIH (RKP, RO1 CA127369), Photolitec, LLC (RKP) the Roswell Park Alliance Foundation (RKP) and the NCI Cancer Center Support grant CA016156 to the Roswell Park Comprehensive Cancer Center (RPCCC), Buffalo, is highly appreciated.

## References

1. Benov L. Photodynamic Therapy (2015) Current status and future directions. *Med. Princ. Prat* 24, 14–28.

2. Ethirajan M.Chen Y.Joshi P.Pandey RK (2011) The role of porphyrin chemistry in tumor imaging and photodynamic therapy.Chem. Soc. Review40, 340–362.
3. Kharkwal GB Dharma SK. Doi T.and Hamblin MR (2011) Photodynamic therapy for infections:Clinical applications. Lasers Surg. Med43, 755–767. [PubMed: 22057503]
4. Sperandio FF Huang Y-Y Hamblin MR (2013) Antimicrobial PDT to kill gram-negative bacteria. Recent Patents on Anti-infective Drug Discovery. 8, 2, DOI 10:2174/1574891 x 113089990012. [PubMed: 23394186]
5. Liu Y.Qin R.Zatt SA Breukink E.and Hegar M.(2015) Antibacterial photodynamic therapy: Overview of a promising approach to fight antibiotic resistant bacterial infections. Journal of Clinical & Translational Research. 1(3), 140–167. [PubMed: 30873451]
6. Jain M.Zellweger M.van den Bergh H.Cook S.Giraud N.(2017) Photodynamic therapy for the treatment of atherosclerotic plaque: Lost in translation? Cardiovasc. Ther35(2). doi: 10.1111/1755-5922.12238.
7. Keyal U.Bhatta AK Wang XL (2016) PDT for the treatment of different severity of acne: A systematic review.Photodiagnosis & Photodynamic Therapy.14, 191–199.
8. Van den Bergh H.Nowak-Sliwinska P.(2016) On the use of photodynamic therapy, as monotherapy or in combination in the treatment of polypoidal choroidal vasculopathy: An update in Handbook of Photodynamic Therapy (Eds. Pandey KK Kessel D.and Dougherty TJ), World Scientific, New Jersey.
9. dos Ancely Ferreira Santos, Daria Raquel Queiroz de Almeida, Leticia Ferreira Terra, Maurício S, Baptista Leticia Labriola(2019) Photodynamic therapy in cancer treatment – an update review. J Cancer Metastasis Treat. 5, 25.
10. Kadish KM Smith KM Guillard R(Edits) (2010) Handbook of Porphyrin Science,Phototherapy, radio-immunotherapy and imaging, Vol 4(Chapters 16–22), World Scientific, New Jersey.
11. Jarvi MT Patterson M. S. and Wilson B. C. (2012) insights into photodynamic therapy dosimetry: Simultaneous singlet oxygen luminescence and photosensitizer photobleaching measurements. Biophys. J 103(3), 661–671.
12. Lovcinsky M, Borecky J.Kubat P and Jezek J.(1999) Meso-tetraphenylporphyrin in liposomes as a suitable photosensitizer. Gen Physiol. Biophys 18, 107–118. [PubMed: 10517287]
13. Jezek P1, Nekvasil M, Skobisová E, Urbánková E, Jirsa M, Zadinová M, Poucková P, Klepáček I. (2003) Experimental photodynamic therapy with MESO-tetrakisphenylporphyrin (TPP) in liposomes leads to disintegration of human amelanotic melanoma implanted to nude mice. Int. J. Cancer103(5), 693–702. [PubMed: 12494481]
14. Shirasu N.Nam S-O, Kuroki M.(2013) Tumor-targeted photodynamic therapy. Anticancer Research 33(7), 2823–2831. [PubMed: 23780966]
15. Pandey RK Zheng G.(2000) Porphyrins as photosensitizers in photodynamic therapy. The Porphyrin Handbook (Eds. Kadish M, Smith KM and Guillard R), Academic Press, San Diego.
16. Ali H.Van Lier JE (2016) Phthalocyanines in cancer-imaging and therapy in Handbook of Photodynamic Therapy (Eds. Pandey RK, Kessel D.and Dougherty TJ), World Scientific, New Jersey.
17. Zhang J.Jiang C.Longo JPF Azevedo RB Zhang H.Muehlmann LAA (2018) An updated overview on the development of new photosensitizers for anticancer photodynamic therapy. Acta Pharmaceutica Sinica B. 8(2), 137–146. [PubMed: 29719775]
18. Abrahamse H.and Hamblin MR (2017) New photosensitizers for photodynamic therapy. Biochem. J 473(4), 347–364.
19. Williams TM Sibrian-Vazquez M.and Vicente MGH (2016) Design and synthesis of photosensitizer-peptide conjugates in Handbook of Photodynamic therapy (Eds. Pandey RK Kessel D.and Dougherty TJ) World Scientific, New Jersey.
20. Debele T-A Peng S.Tsai H-C (2015) Drug carrier for photodynamic cancer therapy. Int. J. Mol. Sci 16, 22094–22136. [PubMed: 26389879]
21. Baba K.Pudavar HE Roy I.Ohulchanskyy TY Chen Y.Pandey R.and Prasad PN (2007) A new method for delivering a hydrophobic drug for photodynamic therapy using pure nanocrystal form of the drug. Mol. Pharm4(2), 289–297. [PubMed: 17266331]

22. Schwartzberg LS and Navari RM (2018) Safety of Polysorbate80 in the oncology setting. *Advances in Therapy*.35(8), 754–767. [PubMed: 29796927]
23. Bodratti AM and Alexandridis P.(2018) Formulation of poloxamers for drug delivery. *J. Funct. Biomater* 9(11), 1–24.
24. Barry AP and Barry NP (2014) Pluronic block-copolymers in medicine: from chemical and biological versatility to rationalization and clinical advances. *Polymer Chem*.5, 3291–3297
25. Lombardo D.Kiselev MA, Magazu S.and Calabdra P.(2015) Amphiphiles self assembly: Basic concepts and future perspectives of supramolecular approaches. *Advances in Condensed Matter Physics*, article ID 151683.
26. Pucelik B.Arnaut LG Stochel G.and Dabrowski JM (2016) Design of Pluronic-Based Formulation for Enhanced Redaporfin-Photodynamic Therapy against Pigmented Melanoma *ACS Appl. Mater. Interfaces* 8, 34, DOI 2203922055.
27. Alakhov V.Klinski E.Shengmin L.Pietrzynski G.Venne A.Batrakova E.Bronitch T.and Kabanov A.(1999) Block copolymer-based formulation of doxorubicin. From cell screen to clinical trials. *Colloids and Surfaces B: Biointerfaces*.16(1), 113–134.
28. Mu C-F Balakrishnan P.Cui F-D Yin Y-M Lee Y-B Choi H-G Yong CS Chung S-J Shim C-K, Kim S-D (2010) The effects of mixed MPEG-PLA/Pluronic copolymer micelle on the bioavailability and multidrug resistance of docetaxel. *Biomaterials*, 31, 2371–2379. [PubMed: 20031202]
29. Chen L.Sha X.Jiang X.Chen Y.Ren Qand Fang X.(2013) Pluronic P105/127 mixed micelles for the delivery of docetaxel against Taxol-resistant non-small cell lung cancer: optimization and in vivo, in vitro evaluation. *Int. J. Nanomedicine*,8, 73–84. [PubMed: 23319859]
30. Chowdhary R.Chansarkar N.Sharif I.Hioka N.and Dolphin D.(2003) Formulation of benzoporphyrin derivatives in Pluronics. *Photochem. Photobiol*77(3), 299–303. [PubMed: 12685658]
31. Pandey RK Sumlin AB Constantine S.Aoudia M.Potter WR Bellnier DA Henderson BW Rodger MASmith KM and Dougherty TJ (1996) Alkyl ether analogs of chlorophyll-a derivatives: Part 1. Synthesis, photophysical properties and photodynamic efficacy. *Photochem. Photobiol*64(1), 194–204.
32. Ci L.Huang Z.Liu Y.Liu Z.Wei G.Lu W(2017) Amino-functionalized poloxamer 407 (F-127) with both mucoadhesive and thermosensitive properties: preparation, characterization and application in a vaginal drug delivery system. *Acta Pharmaceutica Sinica* B7(5), 593–602.
33. Park H.Na, K. (2013) Conjugation of the photosensitizer Chlorine6 to pluronic127 for enhanced cellular internalization for photodynamic therapy. *Biomaterials*,34(28), 6992–7000. [PubMed: 23777915]
34. Gustafson HH Casper DH Grainger DW and Chandehan H.(2015) Nanoparticle uptake: The phagocyte problem.*Nano Today*. 10(4), 487–510. [PubMed: 26640510]
35. Van Meertoo J.Kaspers GJ Cloos J.(2011) Cell sensitivity assays: The MTT assay. *Methods Mol. Biol* 731, 237–235. [PubMed: 21516412]
36. Kessel D.Luo Y, Deng Y.and Chang CK (1997) The role of subcellular localization in initiation of apoptosis by photodynamic therapy. *Photochem. Photobiol* 65(3), 422–426. [PubMed: 9077123]
37. Zhu S.Yao S.Wu F, Jiang I, Wong KL Zhou J.Wang K.(2017) Platinated porphyrin as a new organelle and nucleus dual-targeted photosensitizer for photodynamic therapy. *Org. Biomol. Chem* 15(27), 5764–5771. [PubMed: 28660264]
38. Castano AP Demidova TN and Hamblin MR (2014) Mechanisms in photodynamic therapy: part one- photosensitizers, photochemistry and cellular localization. *Photodiagnosis Photodyn Ther*. 1(4), 279–273.
39. Kessel D.(2019) Apoptosis, paraptosis and autophagy: Death and survival pathways associated with photodynamic therapy. *Photochem. Photobiol* 95, 119–125. [PubMed: 29882356]
40. Chen B.Pogue BWZhou X.O'Hara JA Solban N.Demidenko E.Hoopes PJ and Hasan T.(2005) Effect of tumor host microenvironment on photodynamic therapy in a rat prostate tumor model. *Clinical Cancer Research*. 11, 720–727. [PubMed: 15701861]
41. Henderson BW Bellnier DA Greco WR Sharma A.Pandey RK Vaughan LA Weishaupt KR and Dougherty TJ (1997) An in vivo quantitative structure activity relationship for a congeneric series



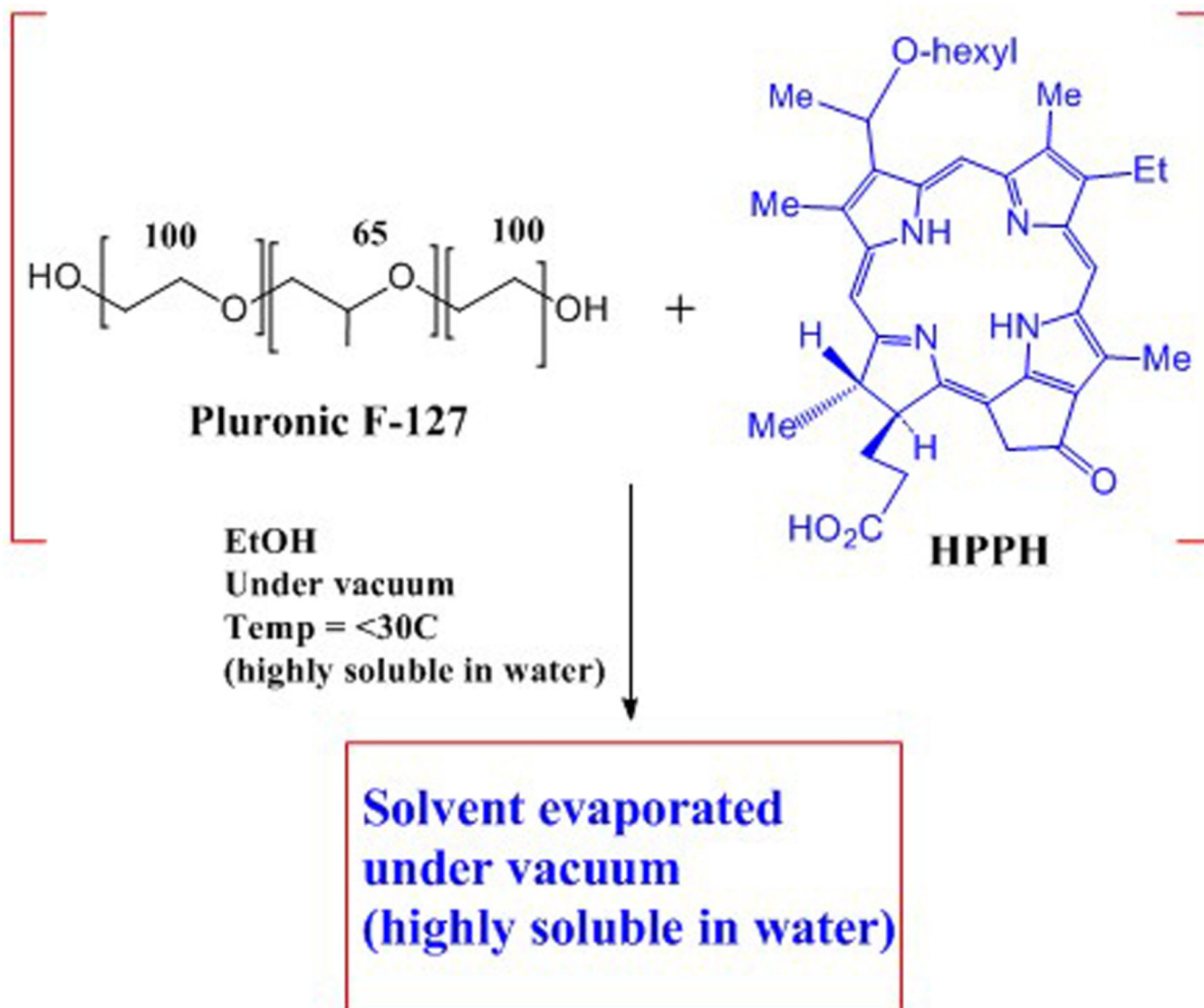
of pyropheophorbide derivatives as photosensitizers for photodynamic therapy. *Cancer Research*, 57(18), 4000–4007. [PubMed: 9307285]

Author Manuscript

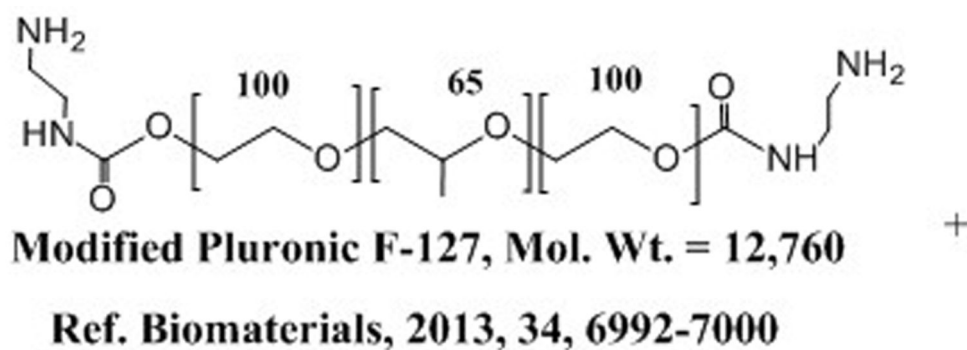
Author Manuscript

Author Manuscript

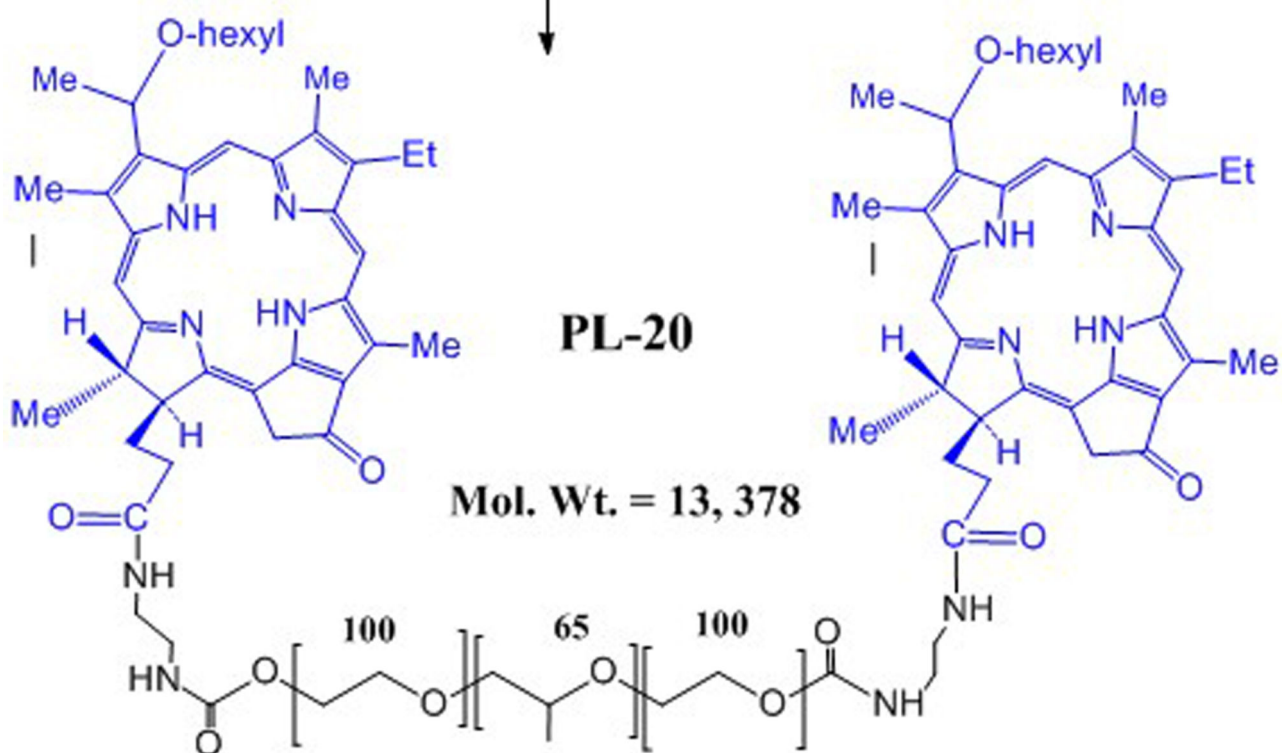
Author Manuscript



**Scheme 1.**  
Method for formulating HPPH in Pluronic F-127.



(i) HPPH, (ii) EDC  
(iii) DMAP, (iv) DCM



**Scheme 2.**  
Synthesis of HPPH-Pluronic F127 conjugate.

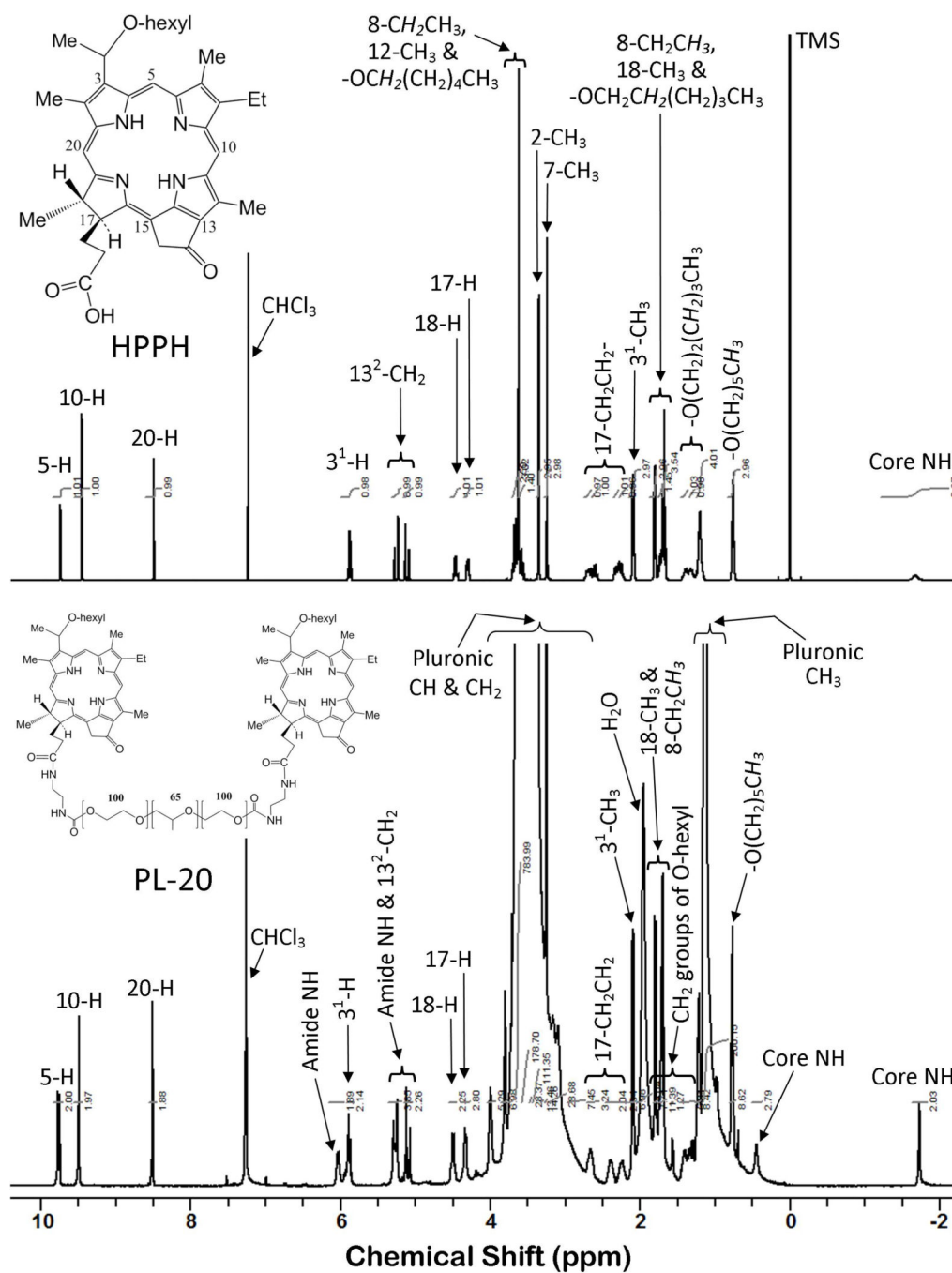


**Figure 1.**

Proton NMR spectra of PL-20 (bottom) and HPPH (top), both in  $\text{CDCl}_3$  solvent. Photosensitizer (PS) resonances of PL-20 are quite similar to those observed for unconjugated HPPH. However, several of these PS peaks were obscured due to interference from large (mainly Pluronic) proton signals. Amide proton peaks at 6.03 and 5.28 ppm are consistent with conjugate formation. Furthermore, the observed ratios of Pluronic to PS peak areas are approximately as expected for PL-20 (two molecules of HPPH are covalently conjugated with amino-Pluronic F-127).

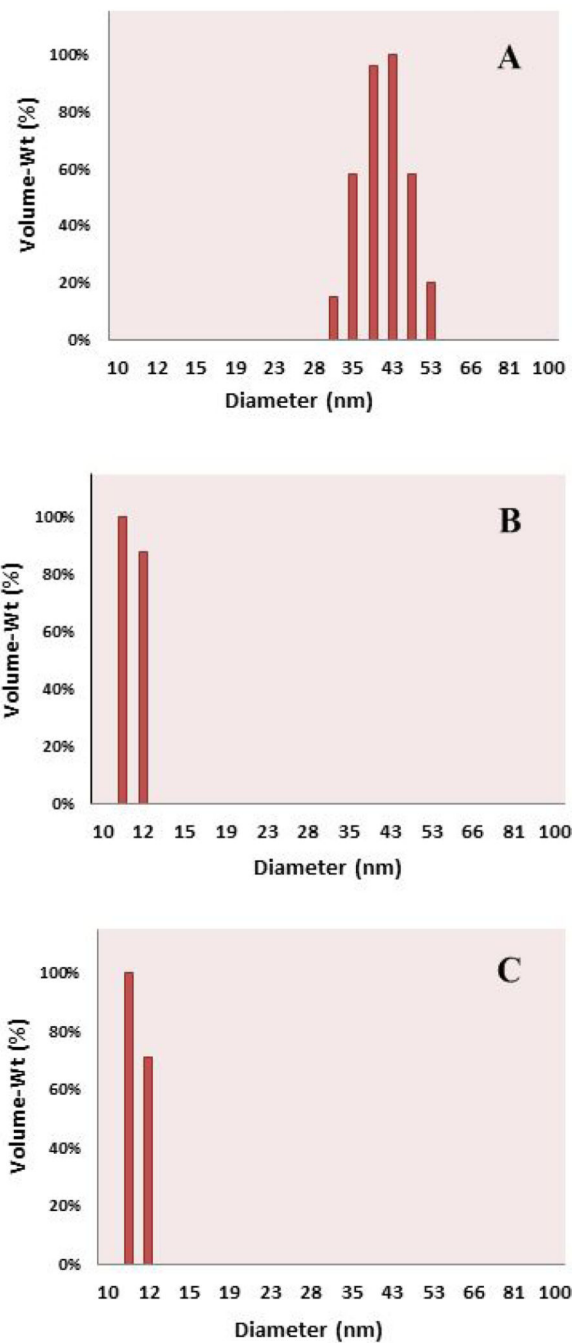


**Figure 2.** Volume-weighted Dynamic Light Scattering (DLS) of (a) HPPH-Pluronic conjugate  $42.1 \pm 4.8$  nm; (b) HPPH-Pluronic F-127 formulation  $11.6 \pm 0.7$  nm; and (c) HPPH-Tween 80 formulation  $11.6 \pm 0.7$  nm. The formulations were filtered through a 0.2 micron syringe filter and immediately read on a DLS Instrument using NICOMP proprietary software.

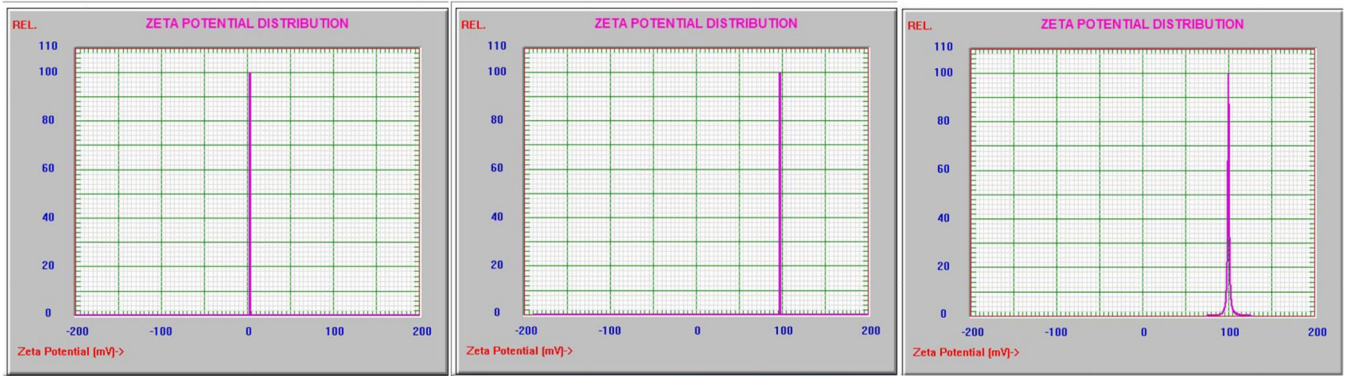


**Figure 3.**  
Zeta Potential ( $\xi$ ) Distribution of (a) 2% Pluronic 127 formulation 0.0 mV; (b) HPPH-Pluronic conjugation +97.57 mV; and (c) HPPH-Pluronic F-127 formulation +100.17 mV.



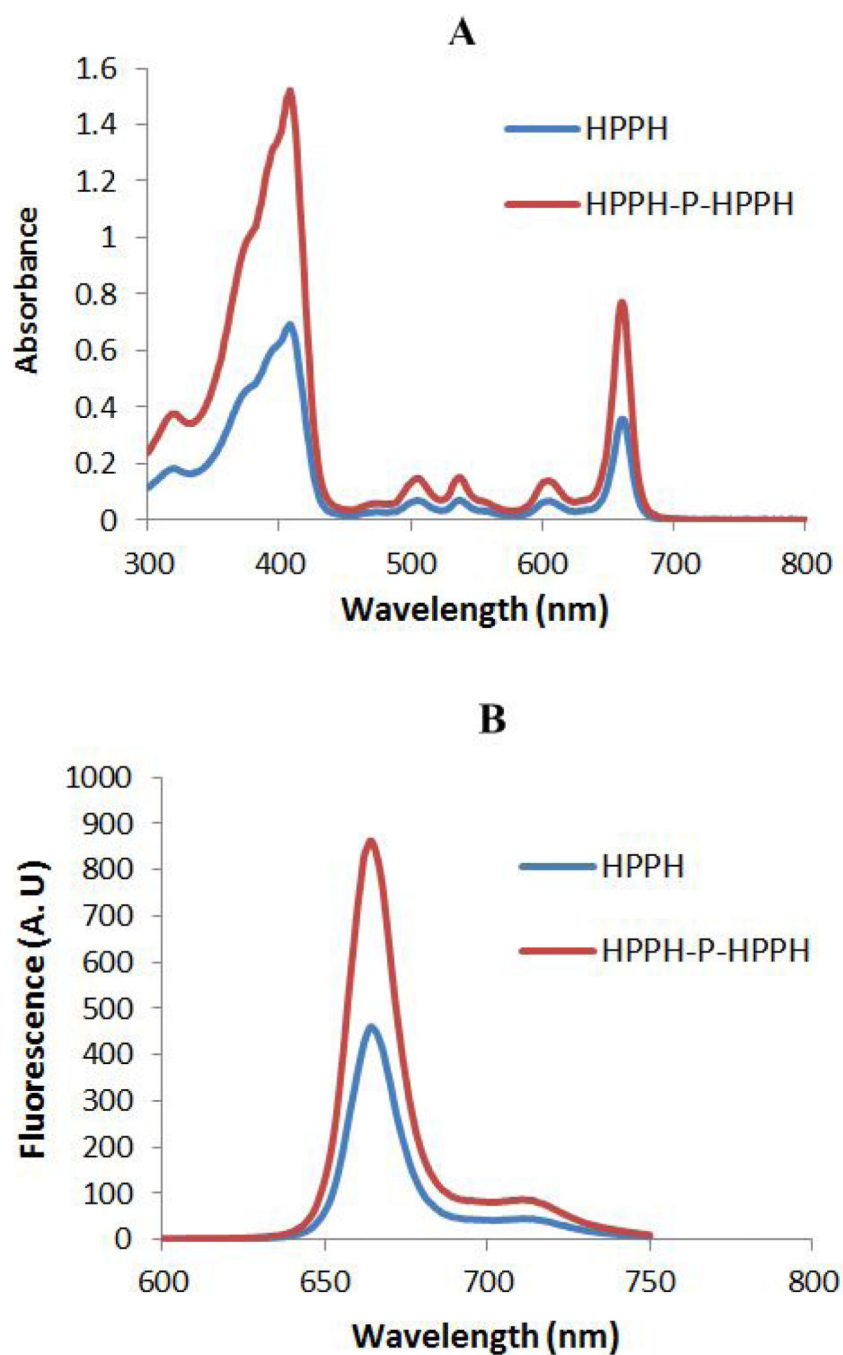


**Figure 4.** (A) Absorption and (B) fluorescence spectra of HPPH and PL-20 (HPPH-P-HPPH) in methanol. The concentration of the solutions used for absorption measurements was 7.5  $\mu\text{M}$ . The concentration of the solutions used for the fluorescence measurements was 0.75  $\mu\text{M}$ .

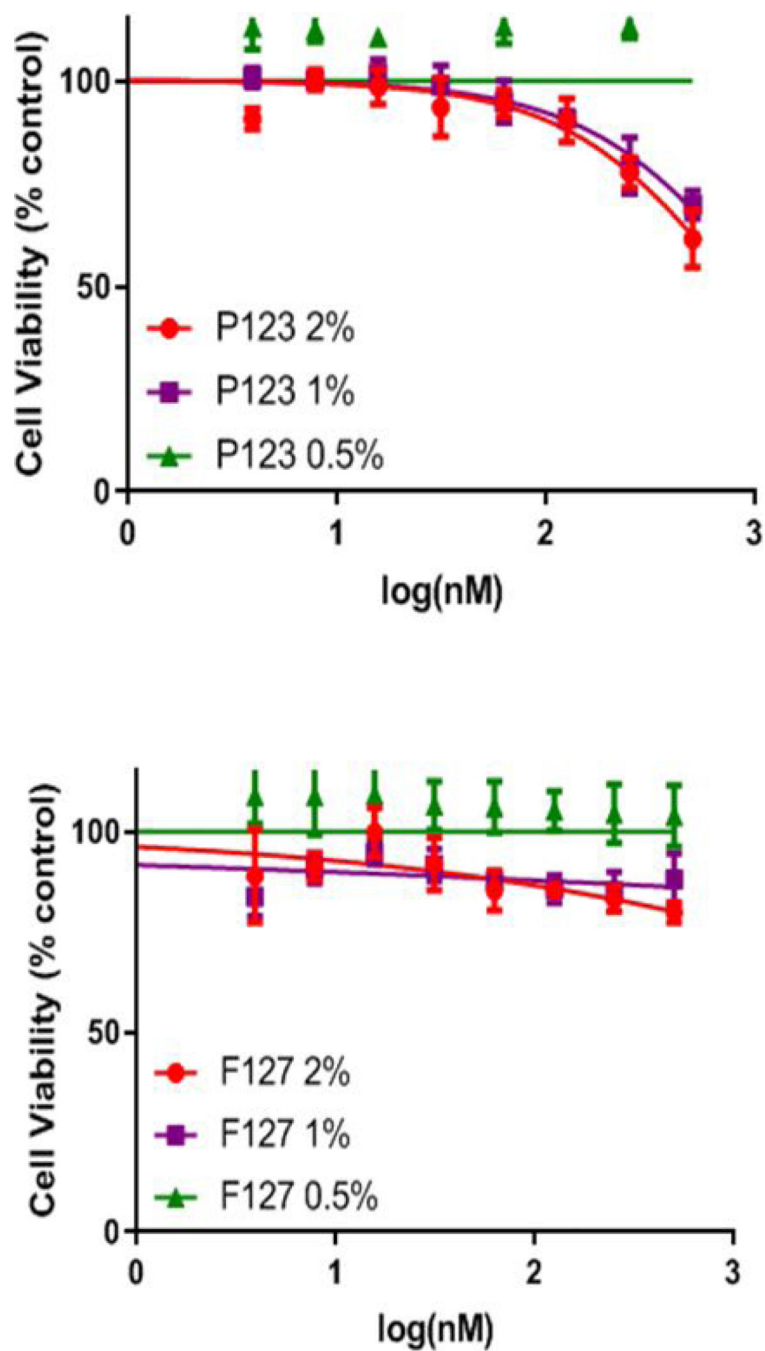


**Figure 5.** *In vitro* cytotoxicity of Pluronic P-123 and F127 formulations over a range of concentrations in Colon26 cells using MTT assay with no light exposure. Pluronic F-127 in DPBS showed no cytotoxicity, Pluronic P-123 showed toxicity at the 1% and 2% Pluronic P-123 concentrations.

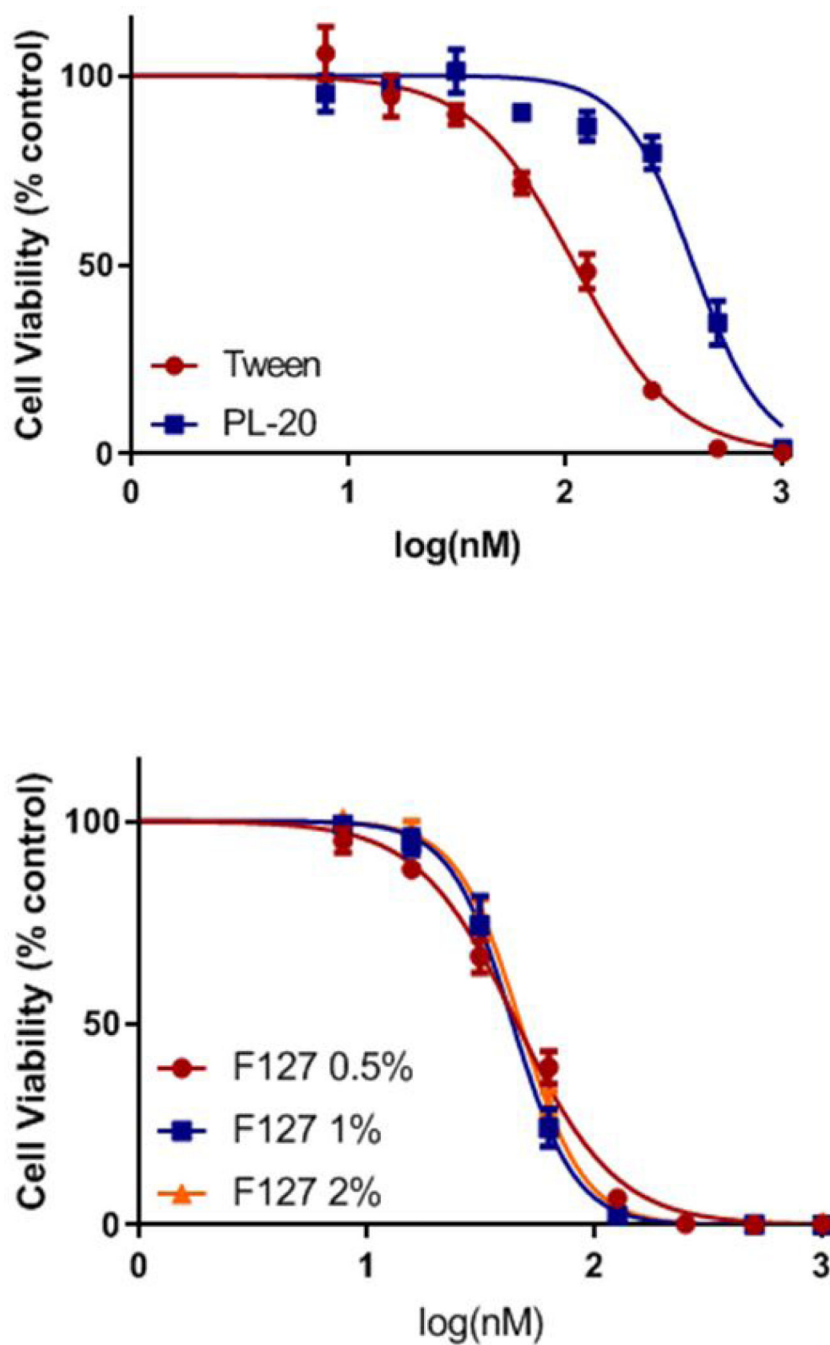


**Figure 6.** *In vitro* photosensitizing activity (MTT assay) of PL-20 PBS and HPPH formulated in Tween 80 Pluronic F127 formulations at variable concentrations, incubated in Ct26 cells for 24h before exposing to a laser light (665 nm) dose of 1 J/cm<sup>2</sup>. The cell viability was determined by MTT assay.

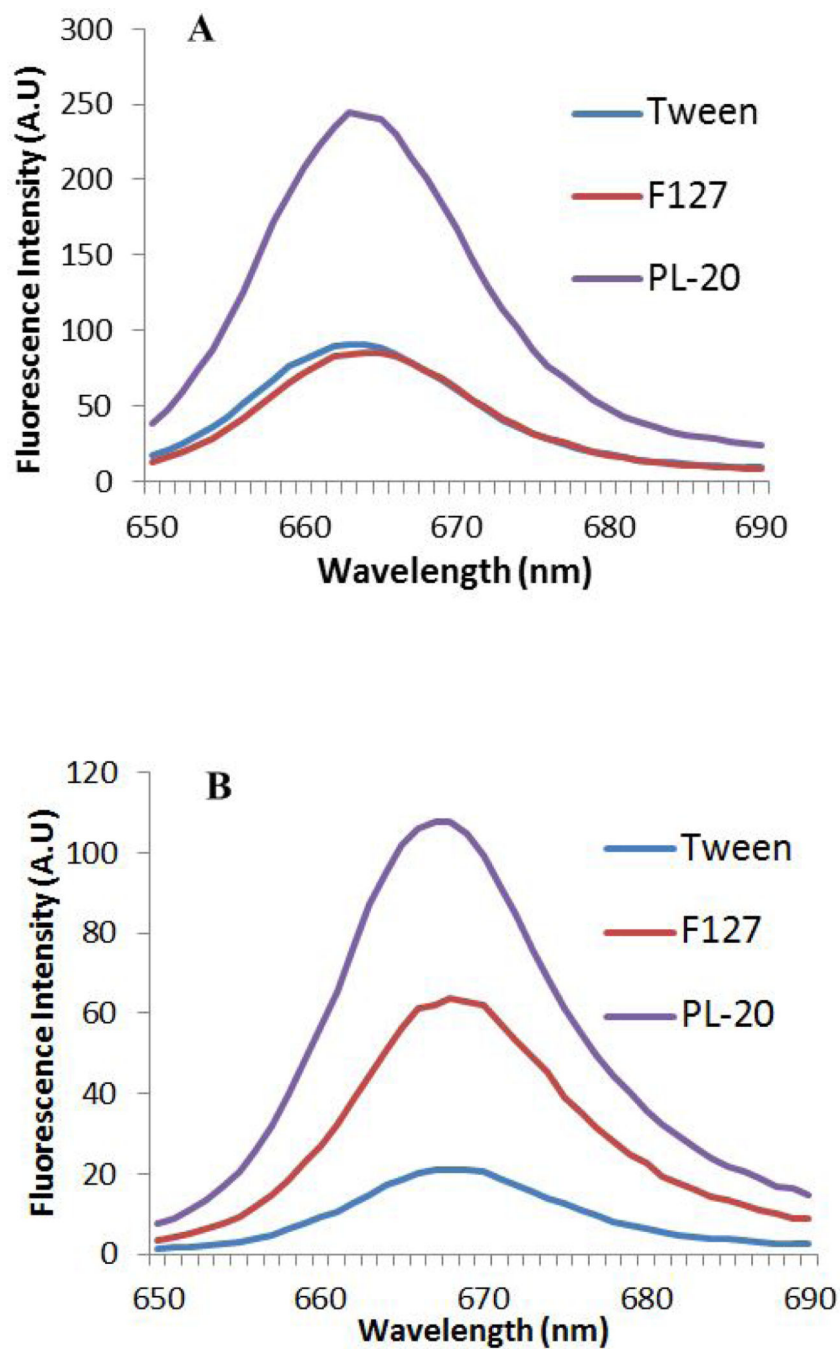


**Figure 7.** Fluorescence intensity of HPPH formulated in various delivery vehicles and PL-20. Graphs were generated using the Cary Fluorimeter. HPPH was dissolved either in methanol (A) or 17% FBS (B) in methanol. Concentration of the PS: 200 nM, excitation wavelength: 407 nm.

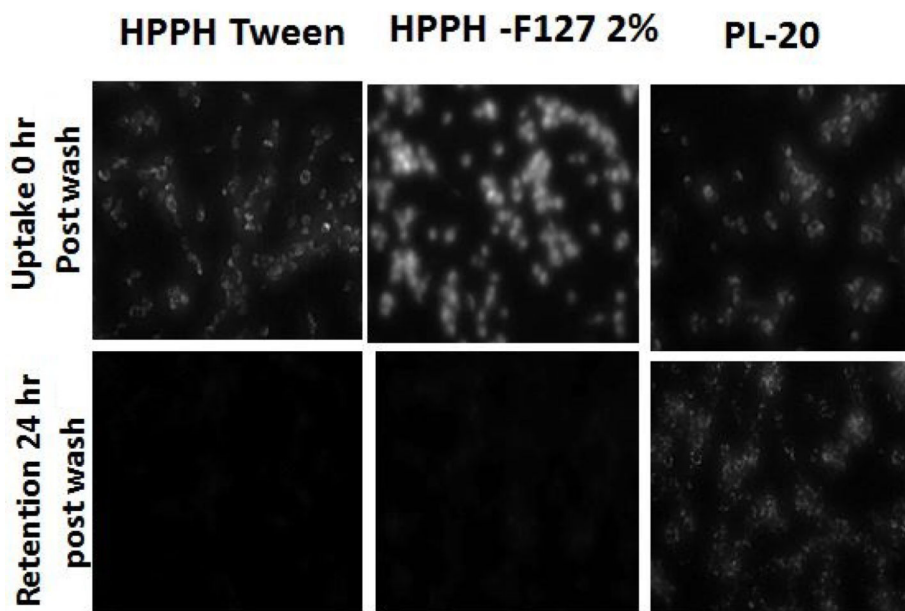
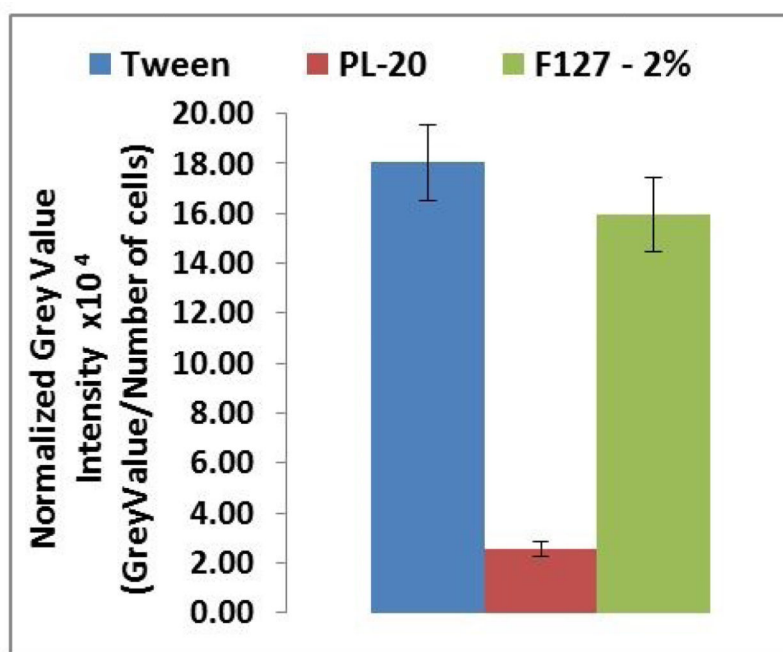


**Figure 8.** (A) *In vitro* uptake of HPPH formulated in Tween 80, Pluronic F-127 (2%) and HPPH-Pluronic conjugate (PL-20) determined by fluorescence microscopy. Ct26 cells were incubated with HPPH in different formulations at a concentration of 500  $\mu$ M for 24 hours, and were washed before measuring the PS fluorescence. Normalized Grey value intensity was derived by dividing the grey value of the image calculated by imageJ by the number of cells in the field (as determined by counting the nuclei stained with Hoechst 33342). (B)

Uptake and retention of HPPH Tween 80, HPPH Pluronic formulations and PL-20 in which two molecules of HPPH are conjugated with Pluronic F-127.

Author Manuscript

Author Manuscript

Author Manuscript

Author Manuscript



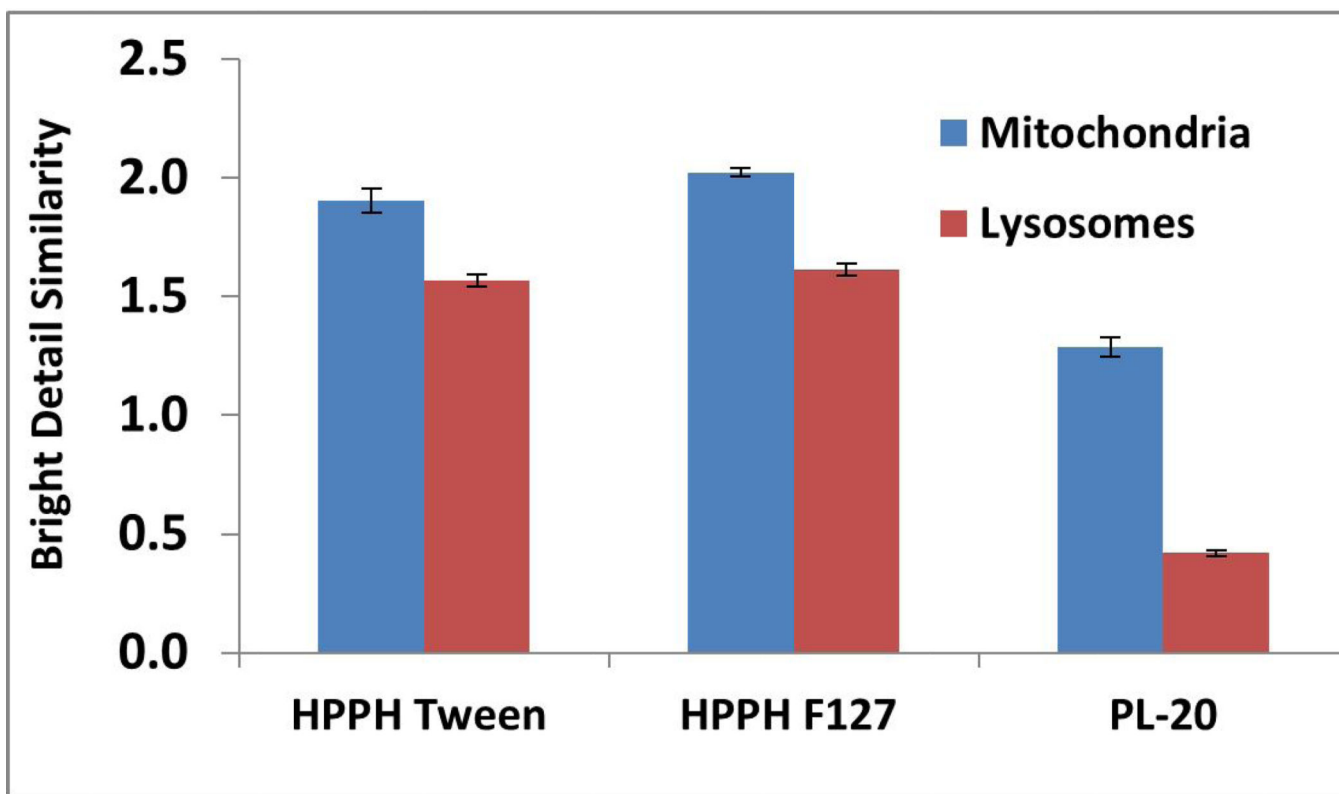


**Figure 9.**  
*In vitro* localization utilizing image stream. HPPH formulations were incubated with Ct26 cells in 6-well plates for 24 hours before Mitotracker red CM0H2Xros and FluoSpheres Green were added to stain the mitochondria and lysosomes, respectively.

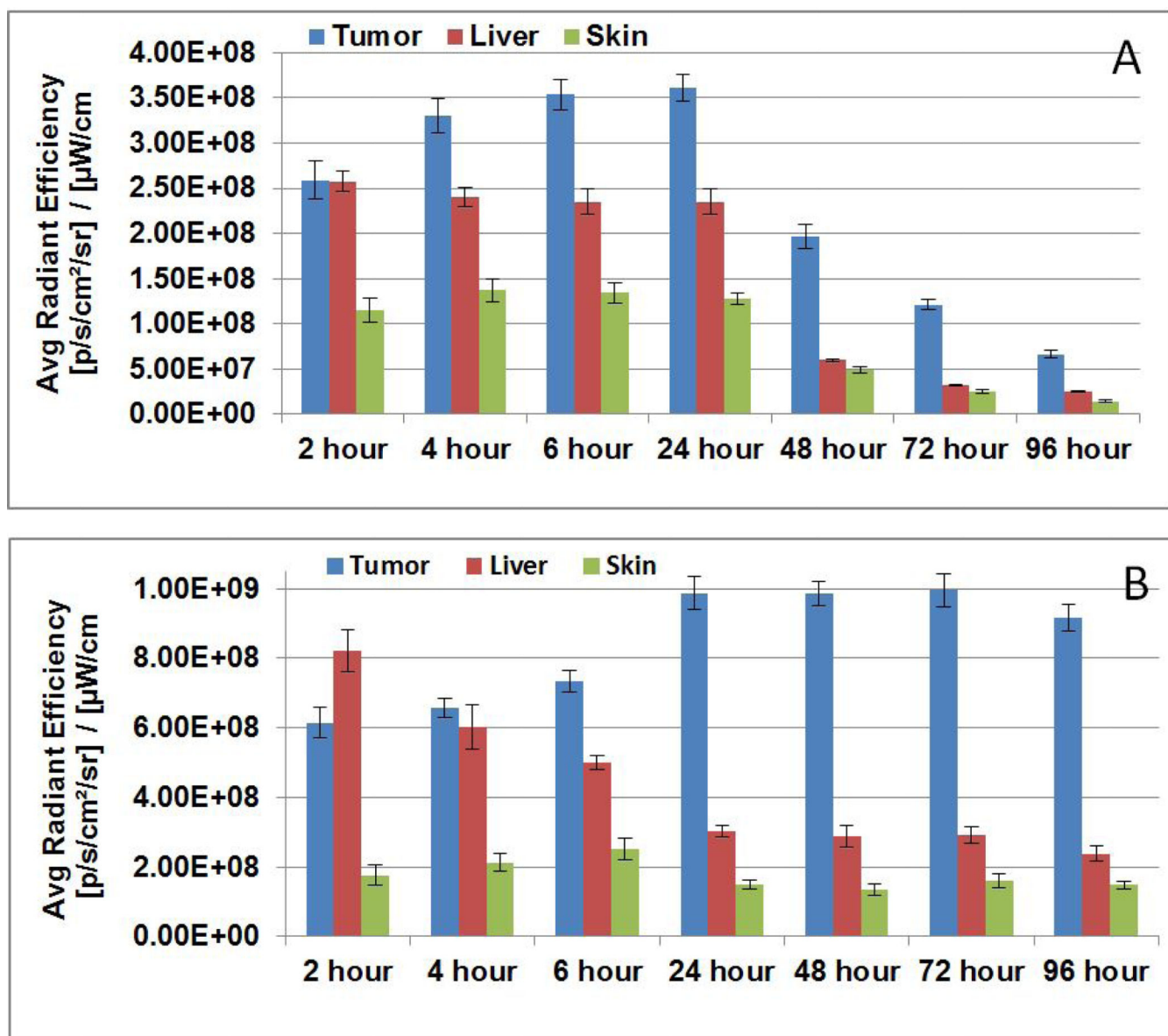


**Figure 10.**

Comparative *in vivo* uptake of HPPH formulated (A) 2% Pluronic F-127 and (B) HPPH-Pluronic F-127 conjugate (PL-20)/PBS in BALB/c mice (3 mice/group/time point) bearing Ct26 tumors. Mice were injected at a dose of 0.47  $\mu\text{mole/kg}$  of the PS and uptake was measured at various time points (2–96h post-injection).

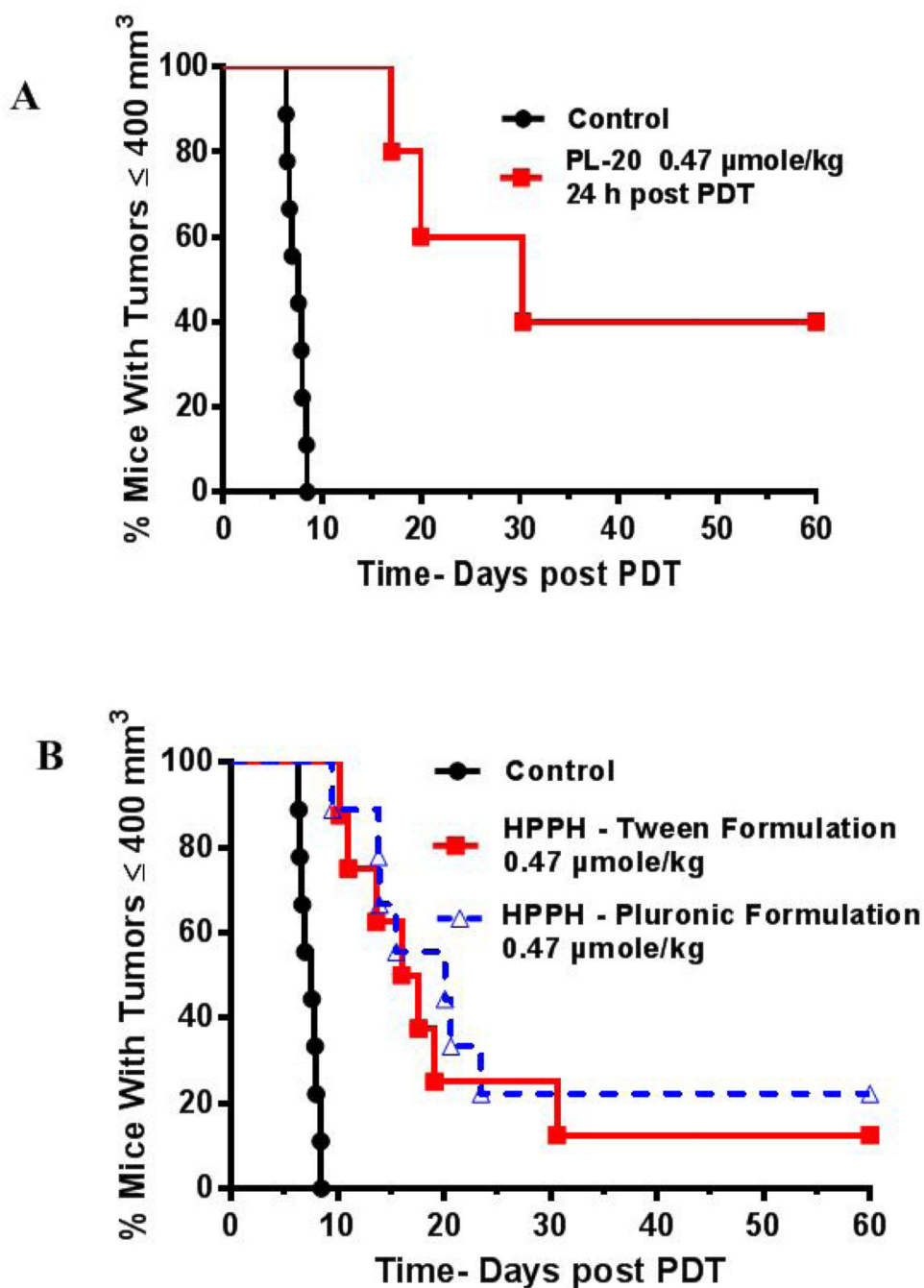


**Figure 11.**

Comparative *in vivo* PDT efficacy of: (A) HPPH conjugated with Pluronic F-127, (B) formulated in Tween 80, Pluronic F-127 and HPPH-Pluronic in BALB/c mice bearing Ct26 tumors at similar treatment parameters. Drug dose 0.47 μmole/kg, light dose: 135 J/cm<sup>2</sup>, 75mW/cm<sup>2</sup>. Tumors were exposed to light at 24h post-injection of the photosensitizers, and tumor growth was measured daily (ref. 41).